

# **BACHELOR-ARBEIT**

vorgelegt an der  
Technischen Hochschule Würzburg-Schweinfurt  
in der Fakultät Informatik und Wirtschaftsinformatik  
zum Abschluss eines Studiums im Studiengang Informatik

## **Simulating Room Acoustics Using Ray Tracing**

Angefertigt an der Fakultät für Informatik und Wirtschaftsinformatik der Technischen  
Hochschule Würzburg-Schweinfurt

Erstprüfer: Prof. Dr.-Ing. Frank Deinzer

Zweitprüfer: Prof. Dr.-Ing. Arndt Balzer

Abgabetermin: 2. 04. 2024

Eingereicht von: Christina Reichel aus Würzburg



Hiermit versichere ich, dass ich die vorgelegte Bachelorarbeit/Masterarbeit selbstständig verfasst und noch nicht anderweitig zu Prüfungszwecken vorgelegt habe. Alle benutzten Quellen und Hilfsmittel sind angegeben, wörtliche und sinngemäße Zitate wurden als solche gekennzeichnet.

Würzburg, den

(Unterschrift)

Hiermit willige ich ein, dass zum Zwecke der Überprüfung auf Plagiate meine vorgelegte Arbeit in digitaler Form an PlagScan übermittelt und diese vorübergehend (max. 5 Jahre) in der von PlagScan geführten Datenbank gespeichert wird, sowie persönliche Daten, die Teil dieser Arbeit sind, dort hinterlegt werden.

Die Einwilligung ist freiwillig. Ohne diese Einwilligung kann unter Entfernung aller persönlichen Angaben und Wahrung der urheberrechtlichen Vorgaben die Plagiatsüberprüfung nicht verhindert werden. Die Einwilligung zur Speicherung und Verwendung der persönlichen Daten kann jederzeit durch Erklärung gegenüber der Fakultät widerrufen werden.

Würzburg, den

(ggf. Unterschrift)

## **Übersicht**

TEXT DEUTSCH

## **Abstract**

TEXT ENGLISCH

# Contents

<b>1</b>	<b>Introduction</b>	<b>1</b>
1.1	Motivation . . . . .	1
1.2	Scope . . . . .	3
<b>2</b>	<b>Interpolating Intersection Checks</b>	<b>5</b>
2.1	Intersection Checks for Spheres . . . . .	6
2.2	Intersection Checks for Surfaces . . . . .	8
2.3	Computational Cost . . . . .	11
2.4	Looping Scenes And Full Algorithm . . . . .	12
<b>3</b>	<b>Time-Based Chunks</b>	<b>13</b>
3.1	Chunks vs. Bounding Volumes . . . . .	13
3.2	Data Structure . . . . .	14
3.3	Calculating Chunks . . . . .	15
3.4	Traversing Chunks . . . . .	15
<b>4</b>	<b>Time-Based Impulse Responses</b>	<b>17</b>
	<b>Bibliography</b>	<b>19</b>
	<b>List of Figures</b>	<b>21</b>
	<b>List of Tables</b>	<b>23</b>



# Chapter 1

## Introduction

### 1.1 Motivation

While there has been plenty of research into simulating sound propagation using both geometric and numerical methods, nearly all of it only concerns itself with static scenes, where neither objects within the scene nor the sound emitter nor receiver move with time.

Simulation of dynamic or moving scenes is mostly unexplored. This is mostly because it is only really relevant for scenarios where objects or receivers can move at speeds within one or two orders of magnitude from the ray's travelling speed; If this condition is not fulfilled, the error introduced from the snapshot method described below becomes minimal enough to be disregarded.

For light, the travelling wave relevant to computer graphics, this condition does not apply as light famously travels at approximately  $3 \cdot 10^8 m/s$ . As a reference, the fastest velocity achieved by humans is approximately  $1.1 \cdot 10^4 m/s$  during the launch of Apollo 10. Seeing as even this extreme case is four orders of magnitude smaller than the speed of light, errors introduced to computer graphics by the snapshot method are especially small.

Only a comparatively small part of the research into ray tracing comes from outside of computer graphics to begin with, and even in other fields, such as acoustics simulation, the error introduced by the snapshot method is only relevant in edge cases. All of this makes simulation of moving scenes a rather niche problem.

Despite this, some research into simulating moving or dynamic scenes' acoustics has been done: Raghuvanshi et al. [10] explore a numerical approach to handle dynamically moving emitters and receivers, but do not look into moving objects within the scene.

Chandak et al. [3] attempt to simulate dynamic scenes in real-time, with support for dynamically moving scenes but sacrificing accuracy. This is less exploring how to handle moving scenes and

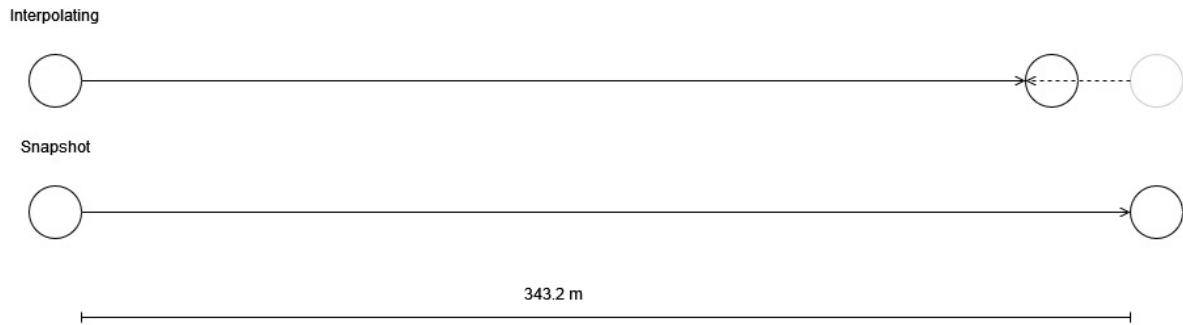


Figure 1.1: Difference between ray travelling distance using the newly developed interpolating method (top) as opposed to the snapshot method (bottom). In the interpolated version, the ray only travels part of the distance as the receiver travels the remainder.

more exploring methods to run acoustics simulation fast enough to re-calculate acoustics at a similar rate to that at which objects move by significant amounts.

Similarly, EAR, an acoustics simulation tool based on the 3d modelling software blender, allows for moving scenes through blender's keyframe system, but is inaccurate for the same reason as Chandak's real-time approach:

Both EAR and Chandak et al. approach the simulation of moving scenes by taking a static version of the scene at the time rays are emitted to create an impulse response, then bouncing rays through this static snapshot. This approach will be called the snapshot method in this thesis. The snapshot method comes with a few advantages: As the snapshot is just a static scene, the same well-explored and -optimised bouncing logic used for static scenes can be copied without changes. Also, crucially, knowledge of how the scene will move over the time the ray spends bouncing around it is not required. All data necessary to simulate the bouncing is available at the time the ray is emitted, without a need for information on how the scene will continue to move. This is especially helpful for real-time simulation of dynamic scenes, as data about how the scene will continue to move is not fully known at runtime.

The major downside of this snapshot approach is that it tends to introduce errors when objects or receivers move at high speeds. As a simple example case, take the scene described in 1.1: A receiver starts 343 meters away from an emitter and moves towards it at  $1/9$ th the speed of sound, roughly 38 meters per second (137.2 kilometers per hour, a speed most modern cars can reach without problems).

Using the snapshot approach, a ray traveling directly from emitter to receiver would arrive after travelling the full 343 meters, taking 1 second for it to arrive at the receiver. In actuality, in the time the ray takes to travel the first 90% of that distance, the receiver has already travelled the



remaining 10%, making for a response time of 0.9 seconds rather than 1 second.

While Bilibashi et al. [2] have attempted to solve this issue, they only aimed to simulate waves bouncing between a few set points, namely cars, rather than simulating full room acoustics. Their vector-based approach cannot be used for a full scene simulation.

To accurately simulate both edge cases occurring in the real world (such as the example above) and hypothetical situations such as the test cases described below, a new method needs to be developed.

## 1.2 Scope

This thesis proposes a method to simulate rays bouncing through arbitrary scenes with moving receivers and/or objects, assuming all movement within the scene is known at time of calculation. An improved way of checking for intersections between rays and objects is developed, accommodating for this new requirement. Optimisations are evaluated and a time-based chunking method is developed to avoid needless intersection checks. Additionally, a method is developed to losslessly and efficiently store the multiple impulse responses created by re-calculating the impulse responses for different points in time. The goal of this research is to simulate effects such as the situation described in 1.1 without errors introduced by the snapshot method as well as recreate the acoustics of a hypothetical, rapidly rotating room. Three test cases are developed for this and compared to an implementation of the snapshot method: An empty scene with the sound receiver approaching the sound emitter at  $1/9$ th the speed of sound, a square room rapidly rotating and a large, L-shaped room also rapidly rotating around one of its ends, with the receiver and emitter both sitting in said end.

Not within the scope of this thesis is a fully accurate simulation including effects such as the differing bouncing behaviour sound waves show at different frequencies. Only a proof of concept that shows that the idea of this new simulation method works is developed.

Side effects of moving scenes, such as sounds emitted by moving objects, are also discarded as they are irrelevant to the changed intersection logic. A note-worthy side effect that gets ignored is mass inertia: The example case where this would become relevant is the inside of a linearly moving enclosed room, such as a driving car. Due to mass inertia, sound waves travelling inside this moving room behave the same as if the car stood still. Since this effect is only relevant in a niche scenario and it can be simulated using a method that ignores movement entirely, it can be ignored for this research.

Real-time applications cannot use this proposed method as it requires knowledge of objects' future movements ahead of time. Further research is required to develop an alternative method

for real-time or dynamic simulations. A real-time approach could work by not calculating the rays' entire movements at emission time, but instead keeping track of all moving rays and incrementally continuing their journey through the now updated scene at recurring intervals.

## Chapter 2

# Interpolating Intersection Checks

To bounce a ray through a scene, checks need to be performed to know which object the ray intersects with (first) and thus bounces off of. These checks are usually done by modelling objects using an equation that describes whether a point is on the object surface or not, then injecting the ray's function into that equation and resolving. With static objects, this check is trivial: The only parameter to resolve for is the intersection time  $t$ , and said parameter only occurs in the ray function, usually making for a first-degree polynomial function.

With moving objects, this check becomes more complicated: The equation still needs to be resolved for  $t$ , but now  $t$  is also part of the surface equation itself. In this chapter, equations are established and solved to perform intersection checks with moving spheres and surfaces, as those two should already be sufficient to simulate most scenes. Resolution for other primitives, such as quadric surfaces, should be derivable using a similar method.

The general scheme for this is as follows: First, the object is modelled in a way where its position (or other parameters) is also a function of  $t$ . Then, like with a normal check, the function modelling the ray is injected into this equation, then resolved. This will, in the examples below, result in a polynomial function of a higher degree (2nd and 3rd for spheres and surfaces, respectively), which can then be resolved. Note that since the resulting polynomial will be of at least 2nd degree, it can have multiple roots. Only roots that take place after the ray's starting time are relevant. Different primitives might also require different checks to filter out invalid roots depending on how they are modelled, the relevant checks for spheres and surfaces will be described below. Of the remaining roots, the first one represents the actual intersection time, the remaining ones can be discarded.

A ray  $R$ 's position at time  $t$ , with  $R$  starting at the point  $P$  at time  $t_0$  and travelling in the direction  $v$  can be defined as follows:

$$R(t) = P + (t - t_0) \cdot v \quad (2.1)$$

Note that unlike with most ray tracing implementations, the magnitude of the direction vector  $v$  is significant: Since the movement of objects checked for intersections is also dependent on time, objects and the ray must move at the same time scale.  $v$  must accordingly be scaled to fit the velocity of the ray and the implementation's scale for  $t$  and coordinates. Otherwise, the intersection calculation will yield incorrect results as at the resulting intersection times, the ray will either not have travelled to the resulting intersection point yet or will have already surpassed it.

## 2.1 Intersection Checks for Spheres

A sphere  $C$  is modelled as having a radius  $r$  and a collection of keyframes  $k_n$ , each with a center point  $c_{k_n}$  and a time  $t_{k_n}$ . Intersection calculations need to be run separately for each set of consecutive keyframes  $k_1$  and  $k_2$ .

The center point  $c_t$  of  $C$  at time  $t$  can be defined as

$$c_t = m \cdot c_{k_1} + (1 - m) \cdot c_{k_2} \quad (2.2)$$

With  $m$  representing the interpolation point between the two keyframes. For the scope of this thesis, linear interpolation is used, leading to  $m$  being defined as

$$m = \frac{t_{k_2} - t}{\delta t} \quad (2.3)$$

with

$$\delta t = t_{k_2} - t_{k_1} \quad (2.4)$$

For non-linear interpolation modes between two keyframes (such as using a sinusoidal function),  $m$  is defined differently. The math below is still the same until (2.7) where  $m$  is resolved, at which point the new definition of  $m$  must be substituted instead of the definition above. Resolving from there should be trivial, depending on the definition of  $m$ .

For interpolation modes that work with more than two keyframes (such as splines),  $c_t$  would instead need to be defined using that other interpolation function, and the scope of which set of keyframes applies to which range of  $t$  would need to be limited accordingly. Exploring this is

outside the scope of this thesis.

For any given time  $t$ , the surface of  $C$  is then defined as all points  $x$  for which

$$\|x - c_t\|^2 = r^2 \quad (2.5)$$

Inserting (2.1) in place of  $x$  in (2.5):

$$\|P + (t - t_0) \cdot v - c_t\|^2 = r^2 \quad (2.6)$$

$$(P - c_{k_2} + t \cdot v - t_0 \cdot v + m \cdot (c_{k_2} - c_{k_1})) \cdot (P - c_{k_2} + t \cdot v - t_0 \cdot v + m \cdot (c_{k_2} - c_{k_1})) = r^2$$

Resolving this and defining  $\delta c = c_{k_2} - c_{k_1}$  results in a function of  $t$  and  $m$ :

$$\begin{aligned} & \|P - c_{k_2}\|^2 - 2 \cdot t_0 \cdot P \cdot v + 2 \cdot t_0 \cdot c_{k_2} \cdot v + t_0^2 \cdot \|v\|^2 - r^2 \\ & + t \cdot 2 \cdot (P \cdot v - c_{k_2} \cdot v - t_0 \cdot \|v\|^2) + m \cdot 2 \cdot (P \cdot \delta c - c_{k_2} \cdot \delta c - t_0 \cdot v \cdot \delta c) \\ & + t \cdot m \cdot 2 \cdot v \cdot \delta c + t^2 \cdot \|v\|^2 + m^2 \cdot \|\delta c\|^2 \\ & = 0 \end{aligned} \quad (2.7)$$

Now, to get a polynomial function of  $t$ ,  $m$  needs to be resolved. With the linear definition of  $m$  from above, this results in the following equation:

$$\begin{aligned} & \|P - c_{k_2}\|^2 - 2 \cdot t_0 \cdot P \cdot v + 2 \cdot t_0 \cdot c_{k_2} \cdot v + t_0^2 \cdot \|v\|^2 - r^2 \\ & + t \cdot 2 \cdot (P \cdot v - c_{k_2} \cdot v - t_0 \cdot \|v\|^2) + \frac{(t_{k_2} - t) \cdot 2 \cdot (P \cdot \delta c - c_{k_2} \cdot \delta c - t_0 \cdot v \cdot \delta c)}{\delta t} \\ & + \frac{t \cdot (t_{k_2} - t) \cdot 2 \cdot v \cdot \delta c}{\delta t} + t^2 \cdot \|v\|^2 + \frac{(t_{k_2} - t)^2 \cdot \|\delta c\|^2}{\delta t^2} \\ & = 0 \end{aligned}$$

This resolves to a 2nd degree polynomial:

$$d_2 t^2 + d_1 t + t_0 = 0 \quad (2.8)$$

with

$$d_2 = \|v\|^2 \cdot \delta t^2 + \|\delta c\|^2 - 2 \cdot v \cdot \delta c \cdot \delta t \quad (2.9)$$

$$d_1 = 2 \cdot ((P - c_{k_2}) \cdot v \cdot \delta t^2 - t_0 \cdot \|v\|^2 - (P - c_{k_2} - t_0 \cdot v) \cdot \delta c \cdot \delta t + t_{k_2} \cdot v \cdot \delta c \cdot \delta t - t_{k_2} \cdot \|\delta c\|^2) \quad (2.10)$$

$$\begin{aligned} d_0 = & (\|P - c_{k_2}\|^2 + 2 \cdot t_0 \cdot (c_{k_2} - P) \cdot v + t_0^2 \cdot \|v\|^2) \cdot \delta t^2 \\ & + t_{k_2} \cdot 2 \cdot (P - c_{k_2} - t_0 \cdot v) \cdot \delta c \cdot \delta t + t_{k_2}^2 \cdot \|\delta c\|^2 - r^2 \cdot \delta t^2 \end{aligned} \quad (2.11)$$

If  $r$  can also be varied between keyframes, replace  $r^2$  with the according interpolated value  $(m - r_{k_1} + (1 - m)r_{k_2})^2$  and resolve accordingly.

The real roots of this equation represent all times at which the sphere and ray would theoretically intersect. Note that all roots  $t$  where  $t < t_{k_1}$  or  $t > t_{k_2}$  must be discarded because the surface is not described by  $k_1$  and  $k_2$  outside the time frame between them. Additionally, all roots where  $t \leq t_0$  must be discarded as these intersections would happen before the ray started, behind its starting location.

Of the real roots remaining after this filter, the lowest result for  $t$  is the one where the ray and sphere intersect, assuming the ray does not bounce off of a different object before that. The coordinates at which the intersection takes place can be calculated by calculating  $R(t)$ .

## 2.2 Intersection Checks for Surfaces

Similarly to spheres, a polygonal surface  $S$  can also be modelled using a set of keyframes  $k_n$ , each with points  $P_{1..o, k_n}$  for the corners of the surface, with  $o \geq 3$  and  $o$  being consistent between keyframes. As with spheres, intersection calculations need to be run separately for each set of consecutive keyframes  $k_1$  and  $k_2$ .

Using  $m$  from (2.3) with the same caveats, each point  $P_{n,t}$  is calculated as

$$P_{n,t} = m \cdot P_{n,k_1} + (1 - m) \cdot P_{n,k_2}, 1 \leq n \leq o \quad (2.12)$$

Assuming all points of the polygon are within one surface, the surface containing the polygon at any given time  $t$  can be described as the set of all points  $x$  where

$$(x - P_{1,t}) \cdot ((P_{2,t} - P_{1,t}) \times (P_{3,t} - P_{1,t})) = 0 \quad (2.13)$$

Injecting (2.1) into (2.13):

$$(P + t \cdot v - t_0 \cdot v - P_{1,t}) \cdot ((P_{2,t} - P_{1,t}) \times (P_{3,t} - P_{1,t})) = 0 \quad (2.14)$$

Exploiting that the vector cross product is distributive over addition (i.e.  $(x + y) \times z = x \times z + y \times z$ ):

$$(P + t \cdot v - t_0 \cdot v - P_{1,t}) \cdot (P_{2,t} \times P_{3,t} - P_{2,t} \times P_{1,t} - P_{1,t} \times P_{3,t} + P_{1,t} \times P_{1,t})$$

As the cross product of a vector with itself is always 0, the last part can be discarded:

$$(P + t \cdot v - t_0 \cdot v - P_{1,t}) \cdot (P_{2,t} \times P_{3,t} - P_{2,t} \times P_{1,t} - P_{1,t} \times P_{3,t}) \quad (2.15)$$

Each of these cross products should be solved individually before resolving the full equation. Using (2.12):

$$P_{a,t} \times P_{b,t} = ((1 - m) \cdot P_{a,k_2} + m \cdot P_{a,k_1}) \times ((1 - m) \cdot P_{b,k_2} + m \cdot P_{b,k_1}) \quad (2.16)$$

Again exploiting that the cross product is distributive over addition, as well as the fact that with a scalar  $a$ ,  $a \cdot (x \times y) = x \times (a \cdot y)$ , this can be resolved to a polynomial function of  $m$ :

$$\begin{aligned} P_{a,t} \times P_{b,t} &= P_{a,k_2} \times P_{b,k_2} + m \cdot (-2(P_{a,k_2} \times P_{b,k_2}) + (P_{a,k_1} \times P_{b,k_2}) + (P_{a,k_2} \times P_{b,k_1})) \\ &\quad + m^2 \cdot ((P_{a,k_2} \times P_{b,k_2}) - (P_{a,k_1} \times P_{b,k_2}) - (P_{a,k_2} \times P_{b,k_1}) + (P_{a,k_1} \times P_{b,k_1})) \end{aligned} \quad (2.17)$$

As with (2.7), to get a function of  $t$ ,  $m$  needs to be replaced with its definition ((2.3) in this case):

$$\begin{aligned} P_{a,t} \times P_{b,t} &= \\ &P_{a,k_2} \times P_{b,k_2} + \frac{(t_{k_2} - t) \cdot (-2(P_{a,k_2} \times P_{b,k_2}) + (P_{a,k_1} \times P_{b,k_2}) + (P_{a,k_2} \times P_{b,k_1}))}{\delta t} \\ &\quad + \frac{(t_{k_2} - t)^2 \cdot ((P_{a,k_2} \times P_{b,k_2}) - (P_{a,k_1} \times P_{b,k_2}) - (P_{a,k_2} \times P_{b,k_1}) + (P_{a,k_1} \times P_{b,k_1}))}{\delta t^2} \end{aligned}$$

This can be resolved to a second-degree polynomial:

$$P_{a,t} \times P_{b,t} = f_{2,a,b}t^2 + f_{1,a,b}t + f_{0,a,b} \quad (2.18)$$

with

$$f_{2,a,b} = (P_{a,k_2} \times P_{b,k_2}) - (P_{a,k_1} \times P_{b,k_2}) - (P_{a,k_2} \times P_{b,k_1}) + (P_{a,k_1} \times P_{b,k_1}) \quad (2.19)$$

$$\begin{aligned} f_{1,a,b} = & -\delta t \cdot (-2(P_{a,k_2} \times P_{b,k_2}) + (P_{a,k_1} \times P_{b,k_2}) + (P_{a,k_2} \times P_{b,k_1})) \\ & -2 \cdot t_{k_2} \cdot ((P_{a,k_2} \times P_{b,k_2}) - (P_{a,k_1} \times P_{b,k_2}) - (P_{a,k_2} \times P_{b,k_1}) + (P_{a,k_1} \times P_{b,k_1})) \end{aligned} \quad (2.20)$$

$$\begin{aligned} f_{0,a,b} = & \delta t^2 \cdot (P_{a,k_2} \times P_{b,k_2}) \\ & + t_{k_2} \cdot \delta t \cdot (-2(P_{a,k_2} \times P_{b,k_2}) + (P_{a,k_1} \times P_{b,k_2}) + (P_{a,k_2} \times P_{b,k_1})) \\ & + t_{k_2}^2 \cdot ((P_{a,k_2} \times P_{b,k_2}) - (P_{a,k_1} \times P_{b,k_2}) - (P_{a,k_2} \times P_{b,k_1}) + (P_{a,k_1} \times P_{b,k_1})) \end{aligned} \quad (2.21)$$

Inserting (2.18) into (2.15):

$$(P + t \cdot v - t_0 \cdot v - P_{1,t}) \cdot (f_{2,2,3}t^2 + f_{1,2,3}t + f_{0,2,3} - f_{2,2,1}t^2 - f_{1,2,1}t - f_{0,2,1} - f_{2,1,3}t^2 - f_{1,1,3}t - f_{0,1,3}) = 0$$

Introducing  $g_n = f_{n,2,3} - f_{n,2,1} - f_{n,1,3}$  for readability, resolving  $P_{1,t}$  as per (2.12) and introducing  $\delta P_1 = P_{1,k_2} - P_{1,k-1}$ :

$$(P + t \cdot v - t_0 \cdot v - P_{1,k_2} + \frac{t_{k_2} \delta P_1}{\delta t} - \frac{t \cdot \delta P_1}{\delta t}) \cdot (t^2 g_2 + t g_1 + g_0) = 0 \quad (2.22)$$

This can be resolved to a third degree polynomial:

$$t^3 d_3 + t^2 d_2 + t d_1 + d_0 = 0 \quad (2.23)$$

With

$$d_3 = g_2 \cdot v - \frac{g_2 \cdot \delta P_1}{\delta t} \quad (2.24)$$

$$d_2 = g_2 \cdot P - t_0 \cdot g_2 \cdot v - g_2 \cdot P_{1,k_2} + \frac{t_{k_2} \cdot g_2 \cdot \delta P_1}{\delta t} + g_1 \cdot v - \frac{g_1 \cdot \delta P_1}{\delta t} \quad (2.25)$$

$$d_1 = g_1 \cdot P - t_0 \cdot g_1 \cdot v - g_1 \cdot P_{1,k_2} + \frac{t_{k_2} \cdot g_1 \cdot \delta P_1}{\delta t} + g_0 \cdot v - \frac{g_0 \cdot \delta P_1}{\delta t} \quad (2.26)$$

$$d_0 = g_0 \cdot P - t_0 \cdot g_0 \cdot v - g_0 \cdot P_{1,k_2} + \frac{t_{k_2} \cdot g_0 \cdot \delta P_1}{\delta t} \quad (2.27)$$

This polynomial can then be solved using a general cubic formula such as the one described by Abramowitz and Stegun [1] or Flocke's Algorithm [7].

As with spheres, the real roots of this equation are all the points in time at which the ray and the



surface would meet. Roots  $t$  where  $t < t_{k_1}$  or  $t > t_{k_2}$ , as well as roots where  $t \leq t_0$ , must be discarded as explained above.

For the remaining roots, another check needs to be done for whether the intersection point  $R(t)$  is actually inside the polygon, and not just on the same surface. With triangles, this can be trivially done by calculating the homogenous barycentric coordinates  $\alpha, \beta, \gamma$  of  $R(t)$  for  $S$  and verifying that  $0 \leq \alpha \leq 1, 0 \leq \beta \leq 1, 0 \leq \gamma \leq 1, \alpha + \beta + \gamma = 1$ .

The root with the lowest value that satisfies the above conditions again represents the time where the ray and polygon intersect, assuming there is no intersection happening before. If no root satisfies these conditions, no intersection happens.

## 2.3 Computational Cost

To gauge the additional computation cost for interpolated intersection checks as opposed to static ones, consider the analytical solution for static surface intersection calculations, derivation of which (for the ray defined in (2.1) and a surface with at least 3 points  $P_{1..3}$ ) is trivial:

$$t = \frac{(P_1 + t_0 \cdot v - P) \cdot n}{v \cdot n} \quad (2.28)$$

with

$$n = (P_3 - P_1) \times (P_2 - P_1) \quad (2.29)$$

Naively calculating a cross product requires 6 multiplications and 3 subtractions. The dot product requires just 3 multiplications, as does multiplying a scalar onto a coordinate vector. This means that to calculate the intersection time for a static surface, a total of 15 additions/subtractions, 15 multiplications and 1 division is required. As  $n$  is always the same for a surface, it can be cached, reducing the cost to only 6 additions/subtractions, 9 multiplications and 1 division.

For the interpolated surface checks, calculating  $f_{0..2,a,b}$  as per (2.19) to (2.21) alone already takes 71 additions/subtractions and 124 multiplications. As  $g_{0..2}$  takes 3 sets of  $f$ , it thus requires 213 additions/subtractions and 372 multiplications. Since  $g_{0..2}$  remains the same for a pair of surface keyframes independently of the incoming ray, it can be cached for each keyframe pair. The same applies for  $\delta t$  and  $\delta P_1$ , which otherwise would introduce one and three subtractions respectively. Then calculating the surface intersection as per (2.23)-(2.27) requires 14 additions/subtractions, 42 multiplications and 3 divisions, assuming that  $g_{0..2} \cdot v$  and  $\frac{g_{0..2} \cdot \delta P_1}{\delta t}$  are only calculated once each and then reused.

Additionally, this requires resolving the resulting polynomial, the cost of which is implementation dependent, but also rather high compared to the static check. As a reference, the Rust library `roots` used in the proof-of-concept requires 13 additions/subtractions, 58 multiplications and 12 divisions, plus some more complex operations in trigonometric and square/cube root functions.

In total, the amount of calculations, especially multiplications, to perform balloons up with this more complex method. As Whitted already noted in 1980 [12], even in a ray tracing system with static checks, intersection calculations take up the vast majority of processing time (between 75-95% in Whitted's case). Since this effect will only increase with more expensive intersection checks, the amount of intersection checks run per ray should be reduced as much as possible. A method for this will be created in the next chapter.

## 2.4 Looping Scenes And Full Algorithm

# Chapter 3

## Time-Based Chunks

### 3.1 Chunks vs. Bounding Volumes

One common optimisation for ray tracing systems is to limit the amount of intersection calculations by eliminating objects the ray cannot intersect with in a simpler way. There are two general sets of methods used for this:

Bounding Volume Hierarchies (BVHs), first proposed by Clarke [4], work by enclosing each object in the scene within a volume containing it. This bounding volume uses a simpler geometric primitive that allows for faster intersection checks than the object itself, usually quadric surfaces or spheres. These bounding volumes are then grouped into bigger bounding volumes into a hierarchical tree structure. Rays then walk down the tree structure, checking for intersections with the corresponding bounding volumes. If it does not intersect with a branch's bounding volume, any objects within that branch can be ignored for further intersection checks.

Chunks, first proposed as a Three Dimensional Digital Differential Analyzer by Fujimoto and Iwata [6], instead divide a scene into separate cells (chunks), with each chunk keeping a list of which objects are inside it. Rays can then traverse from chunk to chunk along their trajectory and only check for intersections with the objects contained in the chunk they're currently in.

Since objects can move around the scene, using one of these methods without changes becomes inefficient. If, for example, a receiver moves from one end of the scene to the other over the course of ten seconds, its bounding volume would extend over all of that distance for the entirety of the scene, despite it not touching the majority of it for the most part. Similarly, it would be kept in its starting position's chunk for the entirety of the scene despite leaving that area very early, making for needless intersection checks.

For this use case, chunks become a lot more efficient than BVHs: When taking movement over time into account, each object would need separate bounding volumes for separate segments of

time, forcing a ray to not just check one bounding volume, but multiple per object. This also means that in order to be able to create meaningful bounding volume hierarchies, each object's bounding volumes would need to be separated at the same points in time, which can lead to redundancies if objects move at different times. Calculating a useful BVH becomes impossible. The amount of chunks, in turn, does not change: They can be adapted simply by storing not just which objects are inside them, but also when each object enters and exits the chunk. If chunk contents are calculated correctly, this means that no intersection checks take place for objects that aren't inside the given chunk at the given time.

## 3.2 Data Structure

In a simple system, a chunk stores a list where each entry represents an object inside it. To accommodate for objects moving in and out of chunks, entries can instead contain three fields: One containing the index of the object in question, one containing the time at which the object enters the chunk and one containing the time at which the object leaves the chunk. Since the latter two fields might both be optional if the scene starts/ends with the object inside the scene, this can be nicely represented using a sum type such as Rust's Enumerators or C's union types with different states:

```
// Object stays within chunk for the whole scene
// only store the index
Static(object)
// Object enters and exits chunk at the given times
Dynamic(object, time_entry, time_exit)
// Object enters chunk at the given time
// and stays until the end
Final(object, time_entry)
```

As the scene's start time is known and the state of objects before it is irrelevant, a state containing only an exit time is not necessary as it can be modelled using the `Dynamic` state with a `time_entry` matching the scene's starting time. Using a more common product type system, chunk entries can instead be represented as a struct or class where the entry and exit times are optional or nullable fields.

A ray traversing this scene can now simply check when it enters and exits a chunk and pick out the objects to check for intersections with accordingly. When using sum types, the space requirements for static objects only increase by one byte denoting the type's variant (with even

that potentially getting left out, as Herzog showed [9]). For moving objects, only up to two additional fields plus the variant field are required, with the timestamp fields' size depending on the implementation. Compared to the performance gains from avoiding needless intersection checks, this additional space requirement is comparatively minimal.

### **3.3 Calculating Chunks**

### **3.4 Traversing Chunks**



## **Chapter 4**

### **Time-Based Impulse Responses**





# Bibliography

- [ASS48] M. Abramowitz, United States. National Bureau of Standards, and I.A. Stegun. *Handbook of Mathematical Functions with Formulas, Graphs, and Mathematical Tables*. Applied Mathematics Series. U.S. Government Printing Office, 1948.
- [BVD20] D. Bilibashi, E. M. Vitucci, and V. Degli-Esposti. “Dynamic Ray Tracing: Introduction and Concept”. In: *2020 14th European Conference on Antennas and Propagation (EuCAP)*. 2020, pp. 1–5. DOI: 10.23919/EuCAP48036.2020.9135577.
- [Cha08] A. Chandak, C. Lauterbach, M. Taylor, Z. Ren, and D. Manocha. “AD-Frustum: Adaptive Frustum Tracing for Interactive Sound Propagation”. In: *IEEE Transactions on Visualization and Computer Graphics* 14.6 (2008), pp. 1707–1722. DOI: 10.1109/TVCG.2008.111.
- [Cla76] J.H. Clark. “Hierarchical geometric models for visible surface algorithms”. In: *Commun. ACM* 19.10 (Oct. 1976), pp. 547–554. ISSN: 0001-0782. DOI: 10.1145/360349.360354. URL: <https://doi.org/10.1145/360349.360354>.
- [CW88] J.G. Cleary and G. Wyvill. In: *The Visual Computer* 4 (1988), pp. 65–83. DOI: 10.1007/BF01905559.
- [FI85] A. Fujimoto and K. Iwata. “Accelerated Ray Tracing”. In: *Computer Graphics*. Ed. by Tosiya L. Kunii. Tokyo: Springer Japan, 1985, pp. 41–65. ISBN: 978-4-431-68030-7.
- [Flo15] N. Flocke. “Algorithm 954: An Accurate and Efficient Cubic and Quartic Equation Solver for Physical Applications”. In: *ACM Trans. Math. Softw.* 41.4 (Oct. 2015). ISSN: 0098-3500. DOI: 10.1145/2699468. URL: <https://doi.org/10.1145/2699468>.
- [Hav00] V. Havran. “Heuristic Ray Shooting Algorithms”. PhD thesis. Czech Technical University, Prague, Nov. 2000.

- [Her] B. Herzog. *Rust Binary Analysis, Feature By Feature*. <https://research.checkpoint.com/2023/rust-binary-analysis-feature-by-feature/>. Accessed: 2024-02-16.
- [Rag10] N. Raghuvanshi, J. Snyder, R. Mehra, M. Lin, and N. Govindaraju. “Precomputed wave simulation for real-time sound propagation of dynamic sources in complex scenes”. In: *ACM SIGGRAPH 2010 Papers*. SIGGRAPH ’10. Los Angeles, California: Association for Computing Machinery, 2010. ISBN: 9781450302104. DOI: 10.1145/1833349.1778805. URL: <https://doi.org/10.1145/1833349.1778805>.
- [SS15] L. Savioja and U.P. Svensson. “Overview of geometrical room acoustic modeling techniques”. In: *The Journal of the Acoustical Society of America* 138.2 (Aug. 2015), pp. 708–730. ISSN: 0001-4966. DOI: 10.1121/1.4926438. eprint: [https://pubs.aip.org/asa/jasa/article-pdf/138/2/708/13242401/708\\\_1\\\_online.pdf](https://pubs.aip.org/asa/jasa/article-pdf/138/2/708/13242401/708\_1\_online.pdf). URL: <https://doi.org/10.1121/1.4926438>.
- [Whi80] T. Whitted. “An Improved Illumination Model for Shaded Display”. In: *Communications of the ACM* 23.6 (1980), pp. 343–349. DOI: 10.1145/358876.358882.

# List of Figures

1.1	Difference between ray travelling distance using the newly developed interpolating method (top) as opposed to the snapshot method (bottom). In the interpolated version, the ray only travels part of the distance as the receiver travels the remainder. . . . .	2
-----	---	---



## List of Tables

